Available online at www.sciencedirect.com
ScienceDirect
Carbohydrate Polymers 66 (2006) 60–70
Carbohydrate Polymers
www.elsevier.com/locate/carbpol

Effect of fatty acid structure on the morphology of spherulites formed from jet cooked mixtures of fatty acids and defatted cornstarch ☆

George F. Fanta [a,b], Frederick C. Felker [a,b,*], Randal L. Shogren [b], John H. Salch [a,b]

[a] *Cereal Products and Food Science Research Unit, National Center for Agricultural Utilization Research, Agricultural Research Service, United States Department of Agriculture, 1815 N. University St. Peoria, IL 61604, USA*
[b] *Plant Polymer Research Unit, National Center for Agricultural Utilization Research, Agricultural Research Service, United States Department of Agriculture, 1815 N. University St. Peoria, IL 61604, USA*

Received 10 November 2005; received in revised form 3 February 2006; accepted 15 February 2006
Available online 16 May 2006

Abstract

Aqueous mixtures of defatted cornstarch and fatty acids were jet cooked and slowly cooled in order to examine the influence of specific fatty acids on spherulite morphology. Addition of 0.7% palmitic acid yielded a spherulite mixture containing 97% of the torus/disc species, having the expected 6_1 V X-ray diffraction pattern. Linoleic acid, as either the free acid or the partially neutralized sodium salt, yielded spherical/lobed spherulites; and diffraction patterns indicated the 7_1 V conformation. Oleic acid also yielded largely the spherical/lobed species, consistent with its mono-unsaturated structure. The spherulite mixture with palmitic acid varied with both the pH and the amount of palmitic acid used relative to starch. When palmitic acid was partially neutralized with NaOH, significant quantities of spherical/lobed spherulites were observed in addition to the expected torus/disc species. Increasing the amount of free palmitic acid from 0.7% to 2.5%, based on starch, yielded a spherulite mixture containing 77% spherical/lobed particles. Stearic acid yielded a spherulite mixture that contained only 20% of the torus/disc species and 80% of a lobed species that unexpectedly exhibited a 6_1 V diffraction pattern. Myristic acid yielded both torus/disc spherulites and a small, narrow-lobed spherulite species that was almost rod-like in appearance. The fact that different spherulite mixtures were observed with fatty acids having similar chemical structures (and also with the same fatty acid under different experimental conditions) indicates that the influence of fatty acid structure on the conformation of the amylose helix is not the only factor controlling spherulite morphology. The variety of different morphologies observed for these particles under different experimental conditions can be explained by the well-known fact that spherulites are formed from chain-folded, crystalline lamellae that have individual chains of complexed amylose oriented perpendicular to the plane of each lamella. Variables that can affect the formation and growth of crystalline lamellae are considered.
Published by Elsevier Ltd.

Keywords: Starch; Amylose; Fatty acid; Spherulite; Crystallite

1. Introduction

Steam jet cooking is a rapid and continuous process that has been used to prepare aqueous starch dispersions for industrial applications (Klem & Brogley, 1981). As part of our continuing research on starch utilization, we are investigating steam jet cooking as a convenient and inexpensive process for preparing new starch-based compositions.

☆ Names are necessary to report factually on available data; however, the USDA neither guarantees nor warrants the standard of the product, and the use of the name by the USDA implies no approval of the product to the exclusion of others that may also be suitable.

* Corresponding author. Tel.: +1 309 681 6356; fax: +1 309 681 6685.
E-mail address: felkerfc@ncaur.usda.gov (F.C. Felker).

0144-8617/$ - see front matter Published by Elsevier Ltd.
doi:10.1016/j.carbpol.2006.02.017

In the course of these investigations, we have observed the formation of spherulites in dispersions of native lipid-containing starch when these starch dispersions were jet cooked and then allowed to slowly cool. The formation of starch spherulites of this type was also reported by other workers, for example, Davies, Miller, and Procter (1980), Heinemann, Escher, and Conde-Petit (2003), Heinemann, Zinsli, Escher, and Conde-Petit (2003). In a previous study (Fanta, Felker, & Shogren, 2002), we showed that spherulites formed in 4% dispersions of jet cooked cornstarch typically contained two distinct species that differed in size, morphology, and crystal structure. Both types were strongly birefringent and were composed almost exclusively of amylose. The smaller-sized spherulites were disc or torus-shaped; whereas the larger particles were more spherical and sometimes had a 2-lobed or 4-lobed appearance. We have examined the formation of these particles at various stages of the cooling period and have concluded that some of the variations in morphology between the different spherulite types in the large-particle fraction may be ascribed to different stages of spherulite growth. X-ray powder diffraction patterns of the small-particle material matched patterns previously reported for the 6_1 amylose V-helical complex in the hydrated form; whereas diffraction patterns for the larger spherulites suggested the 7_1 V-helical conformation for amylose. These results are consistent with the conclusion of Davies et al. (1980) that these spherulites result from crystallization of helical inclusion complexes formed from amylose and the small amount of native lipids normally present in cornstarch. The complexed native lipids in both the torus/disc and the spherical/lobed spherulite species have been identified (Peterson, Fanta, Adlof, & Felker, 2005).

The present study was carried out to determine whether spherulites having a single structure and morphology (as opposed to a mixture of spherulites) would be formed in jet cooked starch dispersions if the native lipids normally present in commercial cornstarch were extracted and then replaced with a single pure fatty acid. Since palmitic, linoleic. and oleic acids comprise the major portion of the native lipid present in cornstarch granules (Morrison, 1988), these acids were examined initially. To determine the effect of chain length of saturated fatty acids on spherulite morphology, myristic acid (C14) and stearic acid (C18) were also included in this study.

2. Materials and methods

2.1. Materials

Normal, unmodified, food grade cornstarch was a product of A.E. Staley Mfg. Co., Decatur, IL. Percent moisture was determined by vacuum drying accurately weighed starch samples at 100 °C, and all weights of starch are given on a dry weight basis. Starch was defatted by extraction with refluxing 85% methanol–water followed by refluxing 75% *n*-propanol–water (Fanta, Felker, Shogren, & Knutson, 2001).

Fatty acids were obtained from Sigma Chemical Co., St. Louis, MO. Purities of palmitic acid, sodium palmitate, oleic acid, and stearic acid were approximately 99%. The purities of linoleic acid and myristic acids were 99% minimum and 99–100%, respectively.

2.2. Jet cooking starch–fatty acid mixtures and isolation of spherulites

The following two methods were used to prepare starch–fatty acid mixtures for steam jet cooking:

Method A. A solution of 0.42 g palmitic acid (0.7% based on starch; 1.638×10^{-3} mol) in about 20 mL ethanol was mixed with 60.0 g of defatted cornstarch, and the ethanol was removed by evaporation. Molar equivalents of other fatty acids were used. The starch–fatty acid mixture was dispersed in 1200 mL of water, and the dispersion was passed through a Penick & Ford Laboratory Model steam jet cooker, operating under excess steam conditions (Klem & Brogley, 1981). Samples were cooked at 140 °C [back pressure: 40 lb/in.^{2} (2.8 kg/cm^2) steam]. The steam line pressure was 65 lb/in.^{2} (4.6 kg/cm^2). Pumping rate of the aqueous starch slurry through the cooker was about 1 L/min. The hot, jet cooked dispersion (about 1 L of a center cut) was collected in a 1 L stainless steel Dewar flask that was pre-heated to 100 °C. Percent solids in jet cooked dispersions were 4.04 ± 0.06%, as determined by freeze-drying.

Method B. A stirred mixture of 0.456 g (1.638×10^{-3} mol) of Na palmitate, 60.0 g of defatted cornstarch, and 900 mL water was heated for 30 min at 85–90 °C and then cooled to 25 °C. The dispersion was acidified with dilute HCl and diluted with water to 1260 mL. The mixture was jet cooked and collected as in Method A.

The Dewar flask containing the hot, jet cooked dispersion was allowed to stand and slowly cool without stirring for 22 h. Temperature during this cooling period was monitored with an OMB TempBook/66 thermocouple data acquisition system purchased from Omega, Stamford, CT. Initial and final temperatures were 92.9 ± 0.8 °C and 49.9 ± 2.8 °C, respectively. Two 300 g portions of the cooled dispersion were diluted with 2700 mL of water, and the resulting dispersions were centrifuged at 3000 rpm ($\approx 2000g$) in a Beckman GS-6KR centrifuge. The precipitated solids were washed with excess water to remove dissolved starch, and a portion of the washed solid was freeze dried to determine yield. The remaining material was fractionated according to particle size by allowing a dilute water dispersion to partially settle, leaving the smaller particles in suspension. Light microscopy was used to monitor the efficiency of the fractionation procedure.

2.3. Scanning electron microscopy (SEM)

Aqueous dispersions of particles (20 μL) were added to 20 mL absolute ethanol, and the solids were allowed to settle. Settled solids were washed with ethanol and critical point dried on aluminum stubs using CO_2. Dried specimens were then sputter coated with Au–Pd and examined with a JEOL 6400 V scanning electron microscope.

2.4. Light microscopy and birefringence

Never-dried samples in water dispersion were observed with a Zeiss Axioskop light microscope (Carl Zeiss, Inc., Thornwood NY) using phase contrast optics. Representative fields were photographed using a Nikon D100 digital camera (Nikon Corp, Tokyo, Japan). Birefringence was observed using crossed polarizing filters and a Zeiss bright field light microscope (Carl Zeiss, Inc., Thornwood, NY). Representative fields were photographed with Polaroid #57 film.

2.5. X-ray diffraction

X-ray diffraction was carried out as described previously (Fanta, Shogren, & Salch, 1999). Freeze-dried samples were equilibrated at 23 °C and 45% relative humidity for 2 days prior to analysis.

2.6. Determination of complexed lipid by FTIR

FTIR analyses were performed on a Nicolet Impact 410 Spectrometer using the Midrange transmission mode. Samples (5 mg) were ground for 4 min. with 200 mg KBr (No. 0016-015 from Spectra-Tech Inc.) in steel vials containing two steel ball pestles. A Wig L Bug Amalgamator, Model 3110-3A, was used to pulverize the samples. A quantity of this first-ground material needed to give 1 mg sample in the final pellet was then ground with about 400 mg KBr for four minutes, and 300 mg of this final ground mixture was then pressed into a clear pellet at 100,000 lb/in.^{2} (7031 kg/cm^2) using a Perkin-Elmer 13 mm die. Spectra were analyzed using Omnic software from Nicolet.

Standards containing 1–9% palmitic acid, stearic acid, oleic acid, and linoleic acid were prepared by dispersing 0.25 g of defatted normal cornstarch in 50 g water in a Waring blender, heating the dispersion to boiling and then adding measured volumes of an ethanol solution of the fatty acid. At least four concentrations of fatty acid were used for each set of standards. The resulting mixtures were blended for 2 min at high speed and then freeze dried.

The CH_2 stretch peak of the fatty acids at 2852 cm^{-1} was used for these determinations after subtracting the contribution of the broader, more intense starch peak at 2929 cm^{-1}. Defatted normal food grade cornstarch was used to obtain the starch spectrum for subtraction. Three methods of analysis were used. In the first method, the absorbance of the 2852 cm^{-1} peak was measured and then normalized to give an absorbance value for 1.0 mg sample. At low fatty acid percentages, these values were proportional to the amount of fatty acid in the starch composite. The second and third methods were based on the ratios of the fatty acid absorbance at 2852 cm^{-1} to the two prominent starch peaks at 1153 and 1024 cm^{-1}, respectively. These two ratios gave similar values for % fatty acid, and the values were also similar to those obtained from the absolute absorbance method. Linear regression was used to generate standard curves for the three methods, and these curves were then used to determine the fatty acid contents of spherulite fractions. Fatty acid percentages obtained by the three methods were averaged, and standard deviations were calculated.

3. Results

Table 1 shows the yields and types of spherulites obtained when defatted cornstarch was steam jet cooked with pure fatty acids. Two methods were used to prepare starch–fatty acid mixtures prior to steam jet cooking. In Method A, the fatty acid was dissolved in ethanol, the solution was blended with dry starch and the ethanol was then allowed to evaporate. In Method B, the sodium salt of the fatty acid was dispersed in water, starch was added and the resulting dispersion was heated to gelatinize the starch. The pH of the resulting dispersion was then adjusted with dilute HCl. In Experiment 1, 0.7% (by weight) palmitic acid, based on starch was used, and (except for Experiment 5) the other fatty acids and their sodium salts were used in molar equivalent amounts. With the exception of Experiments 2 and 5, spherulite yields ranged from 7.7% to 12.2%, based on the initial weight of starch. In Experiment 5, addition of 2.5% palmitic acid, based on starch, increased the yield to 28%. Weight percent fatty acid in selected spherulite fractions was determined by FTIR analysis, and these values are also given in Table 1.

3.1. Palmitic acid

When palmitic acid was added as the free acid (Experiment 1, Table 1), the spherulites formed were almost exclusively the small, torus/disc species. A few lobed particles were observed; however, these amounted to only about 3% of the spherulite mixture and could not be separated in pure form due to aggregates of torus/disc spherulites that settled at about the same rate. SEM and phase contrast micrographs of these two fractions are shown in Figs. 1A–D. When the sodium salt of palmitic acid was jet cooked with starch under the same conditions with no pH adjustment (Experiment 2), the yield of spherulites was less than 0.2%.

Addition of sodium palmitate to defatted starch, followed by gelatinization and adjusting the pH to 5.7 prior to jet cooking (Experiment 3), yielded equal weights of lobed and torus/disc spherulites. Micrographs of these particles are shown in Figs. 1E–H. When the pH was adjusted to 4.4 (Experiment 4), lobed and torus/disc spherulites were

Table 1
Spherulites formed from defatted cornstarch and pure fatty acids

Experiment	Fatty acid	Preparation method[a]	Free acid or Na salt[b]	Spherulite yield, %[c]	Weight ratio of large (spherical/lobed):small (torus/disc) spherulites[d]
1	Palmitic	A	Free acid	10.1	3:97 (4.4 ± 0.3)
2	Palmitic	A[e]	Na salt, pH 7.8	<0.2	–
3	Palmitic	B	Na salt, pH 5.7	9.7	50 (4.9 ± 0.2):50 (4.2 ± 0.3)
4	Palmitic	B	Na salt, pH 4.4	10.4	18 (4.9 ± 0.2):82 (5.5 ± 0.3)
5	Palmitic	A	Free acid, 2.5%	28.0	77 (5.3 ± 0.3):23 (4.4 ± 0.4)
6	Linoleic	A	Free acid	9.0	100 (7.4 ± 0.5):0
7	Linoleic	B	Na salt, pH 4.3	10.7	>99 (6.4 ± 0.2):<1
8	Oleic	A	Free acid	12.2	98 (6.3 ± 0.3[f]):2 (4.9 ± 0.3)
9	Stearic	A	Free acid	10.2	80 (5.3 ± 0.3):20 (5.0 ± 0.2)
10	Myristic	A	Free acid	7.7	2:98

[a] See Section 2.
[b] With the exception of Experiment 5, free palmitic acid was added at a level of 0.7% (by weight) based on total starch. Sodium palmitate and the other fatty acids and their sodium salts were added in molar equivalent amounts. In Experiment 5, palmitic acid was added at a level of 2.5% (by weight) based on total starch.
[c] Percent yields (by weight) are based on total starch.
[d] Fatty acid contents (% by weight), as determined by FTIR, are shown in parentheses.
[e] Sodium palmitate was dissolved in 80:20 ethanol/water.
[f] Oleic acid content of the largest particles in this fraction.

formed in a ratio of 18:82. Micrographs of these spherulites (not shown) were similar to those of spherulites formed at pH 5.7. When palmitic acid was added as the free acid at a level of 2.5% based on starch (Experiment 5), a 28% yield of spherulites was obtained; and the spherulite mixture contained 77% lobed and 23% of the torus/disc species. Micrographs of these fractions (not shown) were similar to the images observed in Experiments 3 and 4.

Fig. 2A shows an X-ray powder diffraction pattern for the torus/disc spherulites formed in Experiment 1, Table 1. The 6_1 V pattern was the same as the pattern observed earlier for this spherulite species (Fanta et al., 2002). Similar diffraction patterns (not shown) were observed for the torus/disc spherulites formed in Experiments 3–5. Diffraction patterns for the lobed spherulites isolated in Experiments 3–5 (shown in Figs. 2B–D, respectively) showed reflections for both the 6_1 V and 7_1 V conformations, suggesting a mixture of these conformations in these materials. (See Fig. 2E for the 7_1 V scattering pattern observed for spherulites obtained from linoleic acid, described below.)

Weight percentages of complexed palmitic acid in the various spherulite fractions obtained in Experiments 1, 3, 4, and 5 all were in the 4–5% range, regardless of the method of preparation, the amount of palmitic acid used relative to starch, and the particular spherulite species analyzed (i.e., spherical/lobed or torus/disc). These values are lower than those reported for the amount of palmitic acid needed to saturate the amylose helix (Raphaelides & Karkalas, 1988), possibly because the amylose complexes in this study were formed under different experimental conditions.

3.2. Linoleic acid

When linoleic acid was used as the free acid (Experiment 6), no torus/disc spherulites were observed, and the spherulites all exhibited the lobed morphology. Phase contrast and SEM images of these lobed particles are shown in Figs. 3A and B.

Addition of linoleic acid as the sodium salt followed by adjustment of the pH to 4.3 (Experiment 7) yielded a few small, torus/disc spherulites; however, these amounted to less than 1% of the total spherulite mixture. The particles in the rapid-settling fraction were larger than those observed with the free acid, and their morphology was more spherical than lobed. Images of these particles are shown in Figs. 3C and D, and images of the torus/disc fraction are shown in Figs. 3E and F.

The spherical/lobed spherulites isolated in Experiments 6 and 7 exhibited the same X-ray diffraction patterns, and these patterns were the same as the 7_1V pattern observed earlier for this spherulite species (Fanta et al., 2002). The diffraction pattern for the spherical particles isolated in Experiment 7 is shown in Fig. 2E. The torus/disc particles in Experiment 7, exhibited a 6_1 V pattern (not shown) that had the same major reflections as the pattern in Fig. 2A for the torus/disc material obtained with palmitic acid. The spherical/lobed particles in Experiments 6 and 7 contained 6% and 7% linoleic acid, by weight.

3.3. Oleic acid

The spherulite mixture obtained with oleic acid (Experiment 8, Table 1) contained only about 2% torus/disc material, the remainder being the spherical/lobed species. Individual particles in the spherical/lobed fraction varied in size and morphology. Phase contrast micrographs of three fractions of this material having different sizes are shown in Figs. 4A–C. An SEM image of the fraction containing the largest of these particles is shown in Fig. 4D. The X-ray diffraction patterns of these three factions

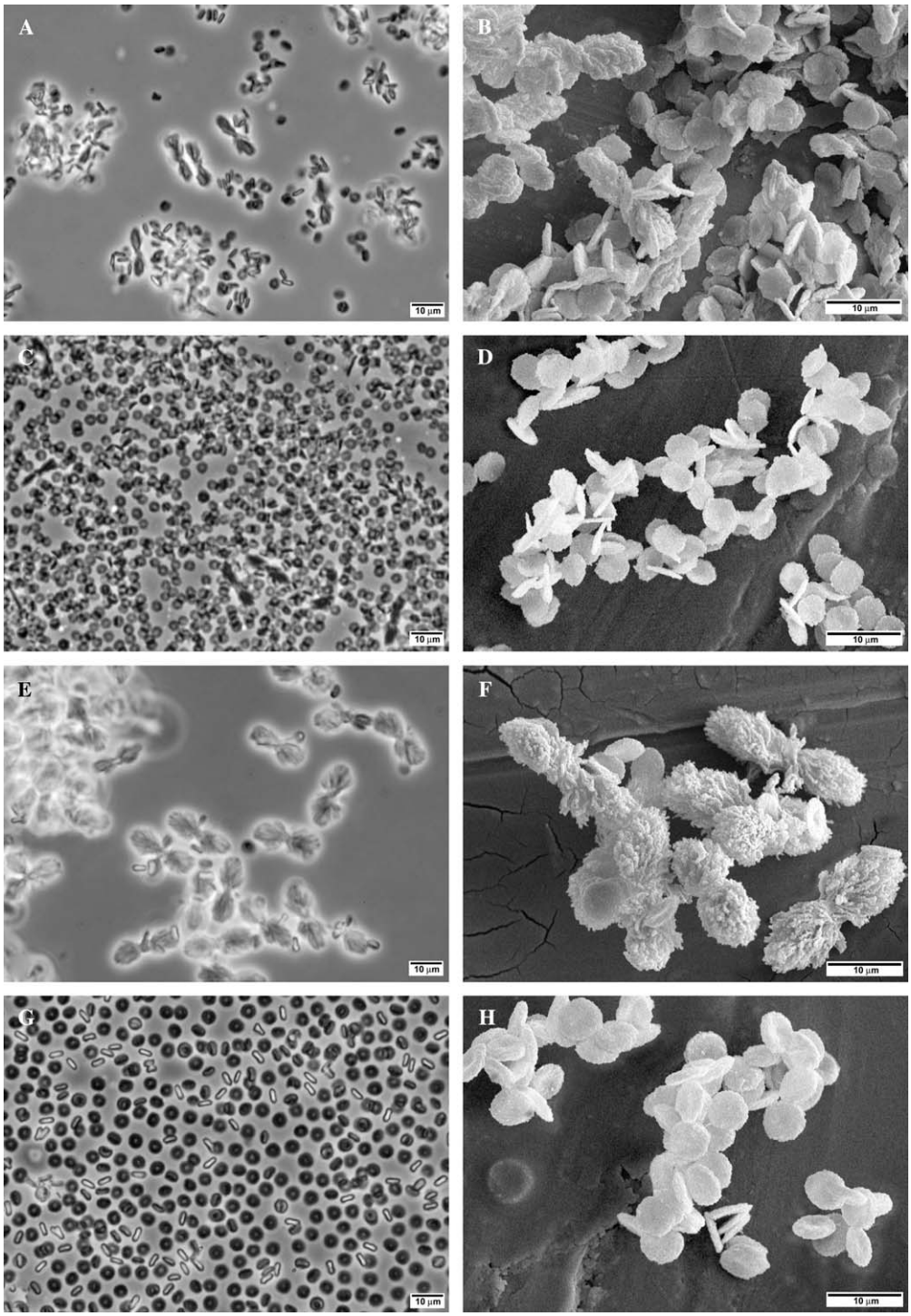

Fig. 1. Micrographs of spherulite fractions formed with palmitic acid. (A), (C), (E), and (G) are phase contrast images. (B), (D), (F), and (H) are SEM images. (A and B) Images of the large (lobed) particle fraction in Experiment 1, Table 1. (C and D) Images of the small (torus/disc) particle fraction in Experiment 1, Table 1. (E and F) Images of the large (lobed) particle fraction in Experiment 3, Table 1. (G and H) Images of the small (torus/disc) particle fraction in Experiment 3, Table 1.

(patterns not shown) were similar to the 7_1 V pattern shown in Fig. 2E. Weight percent complexed oleic acid in the three different size fractions shown in Figs. 4A–C were 5.3 ± 0.2, 5.9 ± 0.1, and 6.3 ± 0.3, respectively.

Micrographs of the torus/disc particles are shown in Figs. 4E and F. Although phase contrast microscopy (Fig. 4E) clearly showed the torus/disc morphology, SEM images were less clear and showed what appeared to be strands of material connecting the individual particles. Also, some clumps of material seemed to be made up of small spheres, less than 1 μm in diameter. These small particles are reminiscent of particles formed from jet cooked

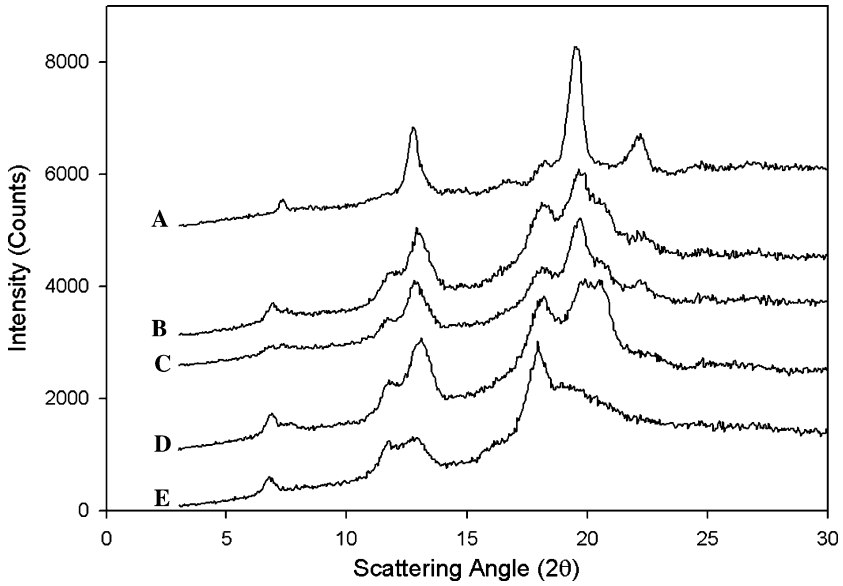

Fig. 2. X-ray powder diffraction scans of spherulite fractions formed with palmitic acid and with linoleic acid. (A) Diffraction scan of the small-particle fraction in Experiment 1, Table 1. (B) Diffraction scan of the large-particle fraction in Experiment 3, Table 1. (C) Diffraction scan of the large-particle fraction in Experiment 4, Table 1. (D) Diffraction scan of the large-particle fraction in Experiment 5, Table 1. (E) Diffraction scan of the large-particle fraction in Experiment 7, Table 1.

native wheat starch (Fanta et al., 2002). The X-ray diffraction pattern of this torus/disc fraction (not shown) was the same as the 6_1V pattern shown in Fig. 2A. This fraction contained 4.9% complexed oleic acid, by weight.

3.4. Stearic acid

The spherulite mixture obtained with stearic acid (Experiment 9, Table 1) contained about 80% lobed material and 20% of the torus/disc species. The lobed particles, shown in Figs. 5A and B, were small relative to the lobed particles isolated in other experiments. Micrographs of the torus/disc particles are shown in Figs. 5C and D. The expected 6_1 V X-ray diffraction pattern was observed for this torus/disc material (Fig. 6A). However, unlike the 7_1 V pattern typically observed for lobed spherulites formed in other experiments, the lobed particles formed with stearic acid showed a 6_1 V pattern (Fig. 6B), although the diffraction peaks were wider than those in Fig. 6A, probably indicating smaller crystallites. Both spherulite fractions contained about 5 % complexed stearic acid, by weight.

3.5. Myristic acid

Phase contrast and SEM images of spherulites obtained with myristic acid (Experiment 10, Table 1) are shown in Fig. 7. About 98% of the spherulites consisted of a mixture of torus/disc spherulites and particles having a thin, lobed appearance (Figs. 7C and D). This small-particle fraction could not be separated into its individual components because of similarities in particle sizes and settling rates. Micrographs of the large-particle fraction (Figs. 7A and B) showed irregularly shaped particles with coarse surface textures. Although both fractions showed 6_1V X-ray diffraction patterns (Fig. 8), the diffraction peaks of the large-particle fraction (Fig. 8B) were broader, probably indicating smaller crystallites.

4. Discussion and conclusions

The goal of this research was to better understand the effect of fatty acid structure on spherulite morphology. We previously observed (Peterson et al., 2005) that both the torus/disc and the spherical/lobed spherulites contained the same mixture of native lipids present in granular cornstarch, although in different relative amounts, especially the palmitic and linoleic acid components. The torus/disc spherulites contained about twice as much palmitic as linoleic acid; whereas these ratios were reversed in the spherical/lobed species. These findings were consistent with the X-ray diffraction patterns observed for these materials. The 6_1 V pattern for the torus/disc species (i.e., 6 glucose units per turn of the helix) suggested the predominance of relatively unhindered straight-chain fatty acids complexed within the amylose helix; whereas the 7_1 V pattern was consistent with a higher percentage of the more sterically hindered linoleic acid. We thus concluded that spherulite morphology was controlled to a large extent by the conformation of the amylose helix, as determined by the structure of the complexed fatty acid.

Initial experiments in the current study supported this conclusion. Addition of 0.7% palmitic acid (free acid) to defatted cornstarch yielded a spherulite mixture containing 97% of the torus/disc species, and the expected 6_1 V diffraction pattern was observed for this material. Also, linoleic acid, as either the free acid or the partially neutralized

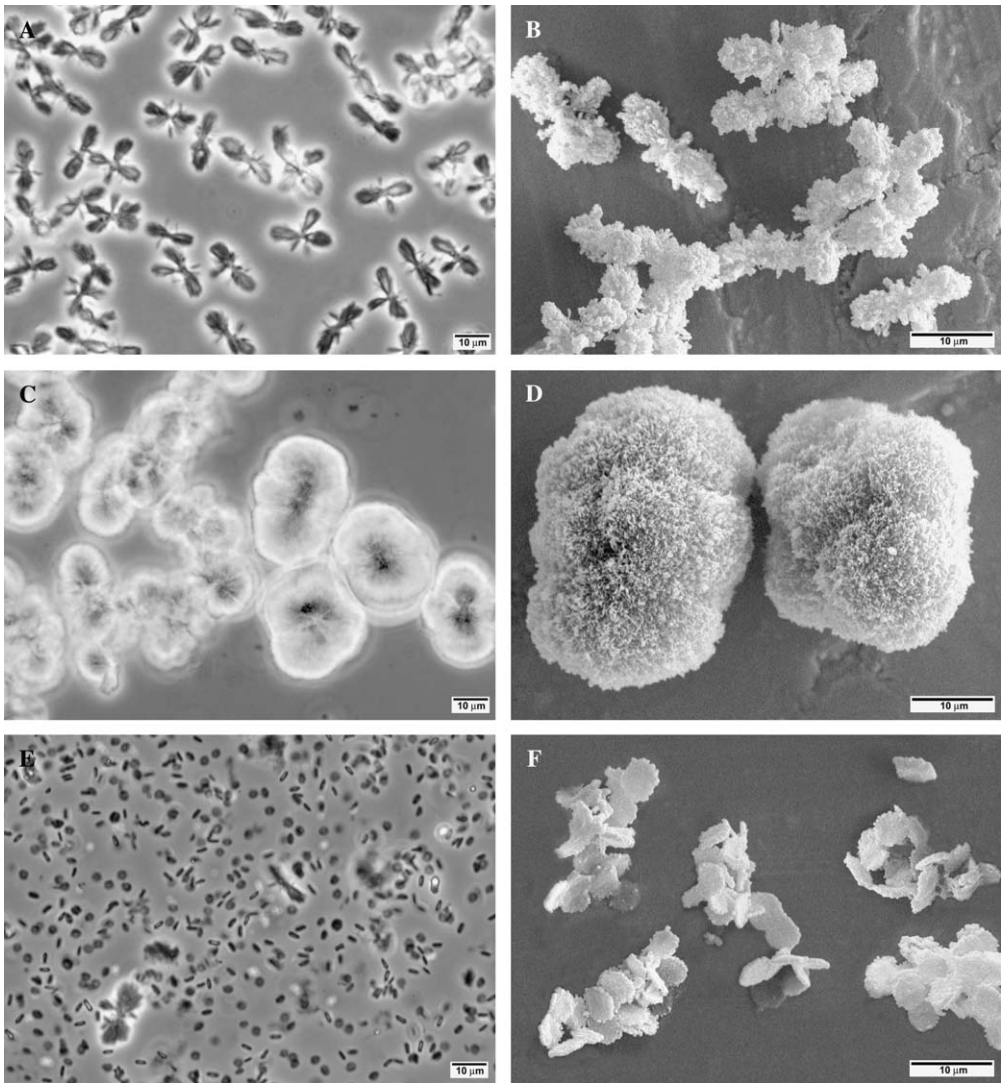

Fig. 3. Micrographs of spherulite fractions formed with linoleic acid. (A), (C), and (E) are phase contrast images. (B), (D), and (F) are SEM images. (A and B) Images of the lobed spherulites formed in Experiment 6, Table 1. (C and D) Images of the large-particle fraction in Experiment 7, Table 1. (E and F) Images of the small-particle fraction in Experiment 7, Table 1.

sodium salt, yielded spherical/lobed spherulites; and as expected, diffraction patterns indicated the 7_1 V conformation. Oleic acid also yielded largely the spherical/lobed species, consistent with its mono-unsaturated structure.

Further experiments, however, showed that the spherulite mixture observed with palmitic acid varied with both the pH of the system and the amount of palmitic acid used relative to starch. When palmitic acid (0.7% level of addition) was partially neutralized with sodium hydroxide, significant quantities of spherical/lobed spherulites (50% and 18% at pHs of 5.7 and 4.4, respectively) were observed in addition to the expected torus/disc species. The diffraction patterns for these spherical/lobed materials suggested a mixture of 6_1 V and 7_1 V conformations. Increasing the amount of free palmitic acid from 0.7% to 2.5%, based on starch, yielded a spherulite mixture containing 77% spherical/lobed particles, and the diffraction pattern of this material was also consistent with a mixture of 6_1 V and 7_1 V conformations. We also observed that stearic and myristic acids, at the same molar concentrations as 0.7%, by weight, palmitic acid yielded spherulite mixtures that were quite different than the mixture obtained with palmitic acid under the same conditions, even though all of these fatty acids were saturated, straight chain materials and differed only in the length of the alkyl chain. Stearic acid yielded a spherulite mixture that contained only 20% of the torus/disc species and 80% of a lobed species that unexpectedly exhibited a 6_1 V diffraction pattern. Myristic acid yielded both torus/disc spherulites and a small, narrow-lobed spherulite species that was almost rod-like in appearance. The fact that different spherulite mixtures were observed with fatty acids having similar chemical structures (and also with the same fatty acid under different experimental conditions) indicates that the influence of fatty acid structure on the conformation of the amylose helix is not the only

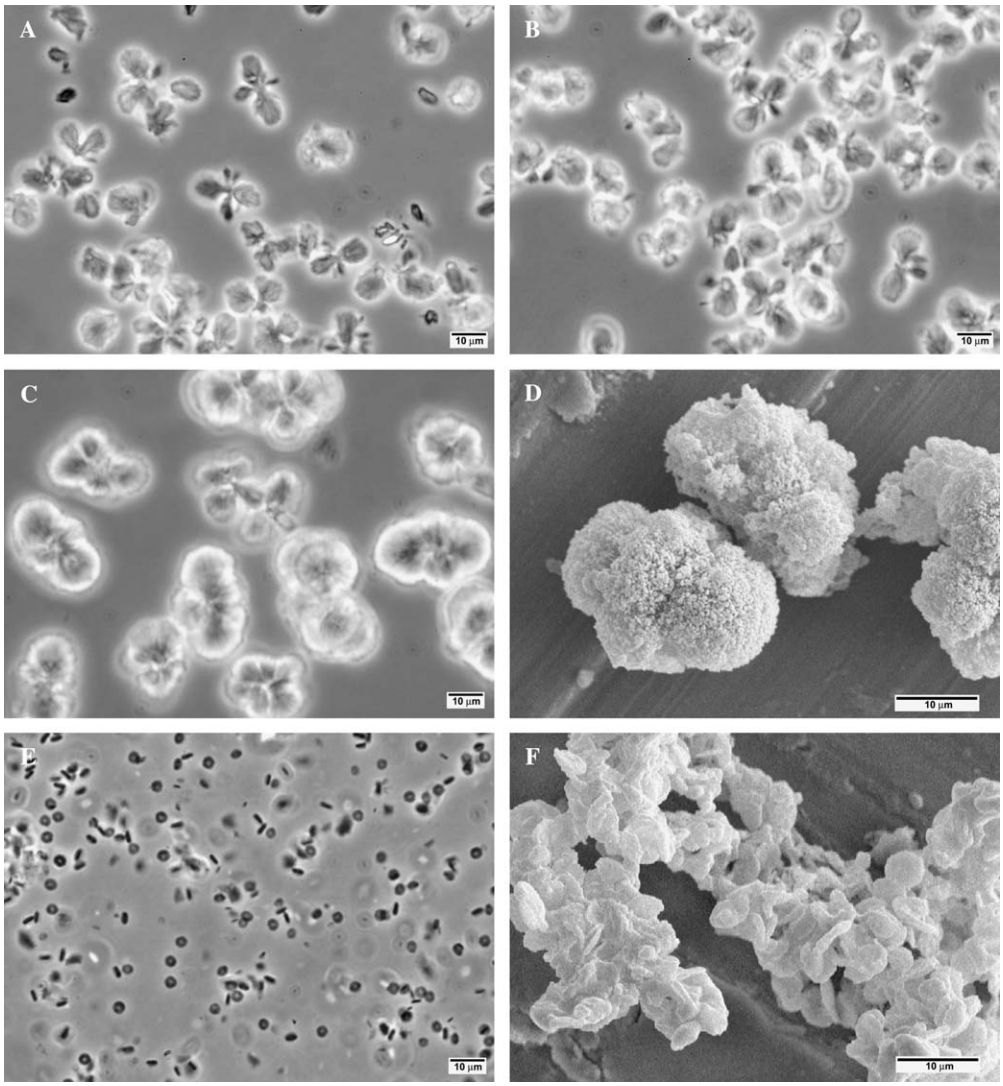

Fig. 4. Micrographs of spherulite fractions formed with oleic acid (Experiment 8, Table 1). (A), (B), (C), and (E) are phase contrast images. (D) and (F) are SEM images. (A) An image of the smallest particles in the large (spherical/lobed) fraction. (B) An image of intermediate-sized particles in the large (spherical/lobed) fraction. (C and D) Images of the largest particles in the spherical/lobed fraction. (E and F) Images of the small (torus/disc) fraction.

factor controlling spherulite morphology. The percentage of fatty acid complexed within the amylose helix is apparently not of major importance in the determination of morphology, since the torus/disc and spherical/lobed particles isolated in each of our experiments contained similar percentages of complexed fatty acids.

The variety of different morphologies observed for these particles under different experimental conditions can be explained by the fact that spherulites are formed from chain-folded, crystalline lamellae that grow (or stack) in a radial direction from a central nucleus. Individual chains of complexed amylose are oriented perpendicular to the plane of each lamella (Manley, 1964; Yamashita, 1965; Yamashita & Hirai, 1966). The spherical morphologies of these spherulites results from branching of lamellae and also from the imperfect stacking of individual lamellae during the growth process. Bassett and co-workers (Abo el Maaty, Hosier, & Bassett, 1998; Bassett, 1999) have proposed that imperfect stacking (or "splaying") of lamellae is due to repulsive forces caused by portions of un-crystallized polymer chains (i.e., "cilia") that are not chain-folded and therefore extend from lamella surfaces. Electron micrographs of spherulites obtained from polyolefins (Bassett, 1984) resembled the spherulite structures observed in this study. Also, Kalinka and Hinrichsen (1997) have published computer simulations of the growth of spherulites from crystalline lamellae and have demonstrated the effects of several different variables on spherulite morphology. Computer-simulated structures obtained by these authors bear a remarkable resemblance to the actual structures observed for the different spherical/lobed particles observed in our studies.

Considering the manner in which these spherulites form, it would be expected that the conformation of the amylose helix (i.e., 6_1 V vs 7_1 V), as determined by

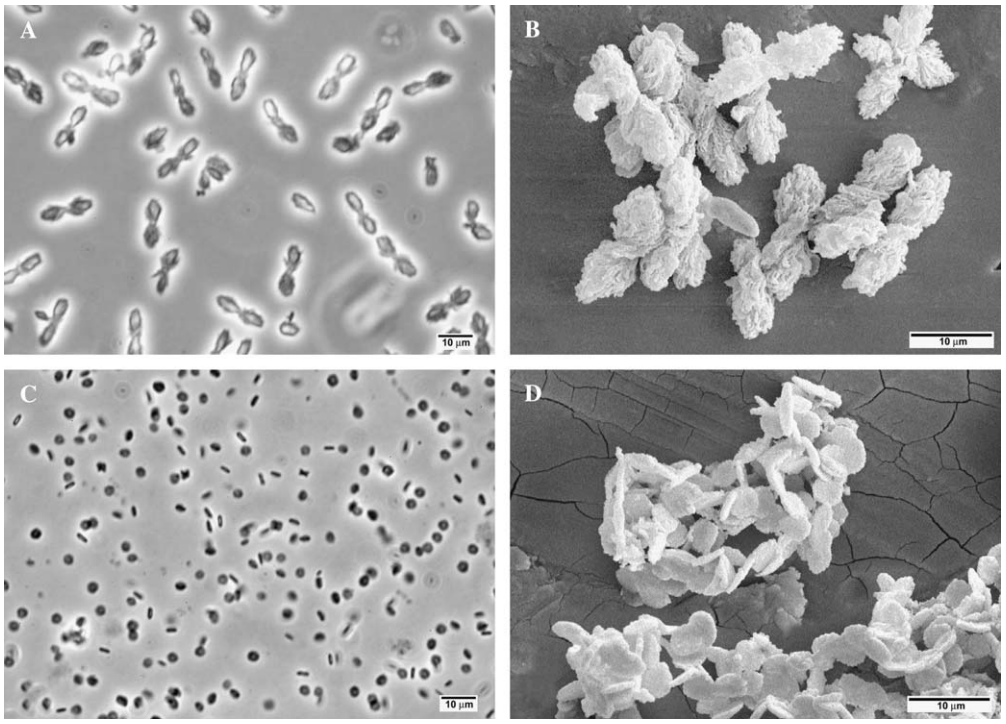

Fig. 5. Micrographs of spherulite fractions formed with stearic acid (Experiment 9, Table 1). (A and C) are phase contrast images. (B and D) are SEM images. (A and B) Images of the lobed spherulites. (C and D) Images of the torus/disc spherulites.

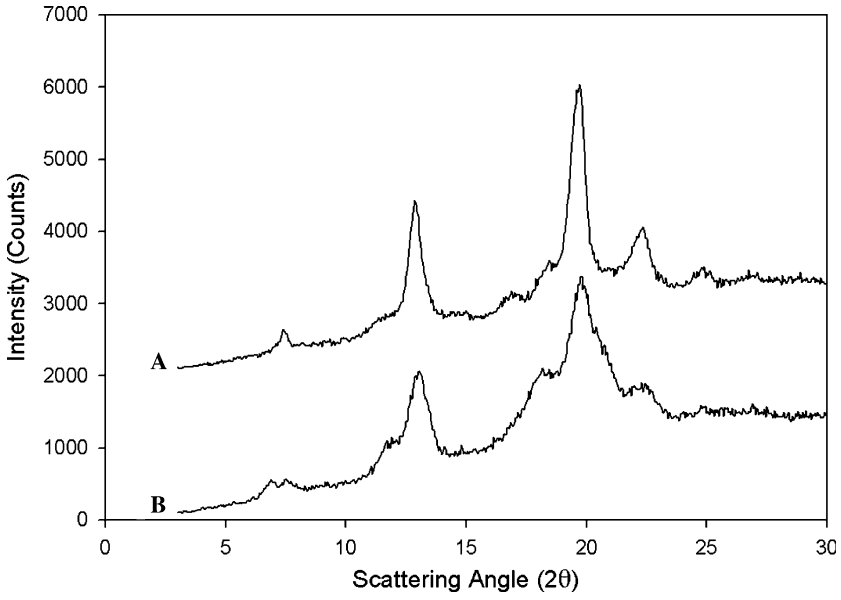

Fig. 6. X-ray powder diffraction scans of spherulites formed with stearic acid (Experiment 9, Table 1). (A) Diffraction scan of the small-particle (torus/disc) fraction. (B) Diffraction scan of the lobed particle fraction.

fatty acid structure, would be a major factor in determining spherulite morphology because of the effect of conformation on chain folding, cilia formation and the branching of lamellae. The question of whether complexes are formed from fatty acid dimers (or other multiples of the fatty acid) within the amylose helix and how these complexed species might affect the conformation of the helix should also be considered. Spherulite morphology can also be influenced by the rate of lamella formation and the rate of spherulite growth, as influenced by the water solubility of the fatty acid (or its sodium salt) in the jet cooked dispersion, the rate at which the dispersions are cooled, and the amount of fatty acid used relative to starch. Bassett (1984) has pointed out the

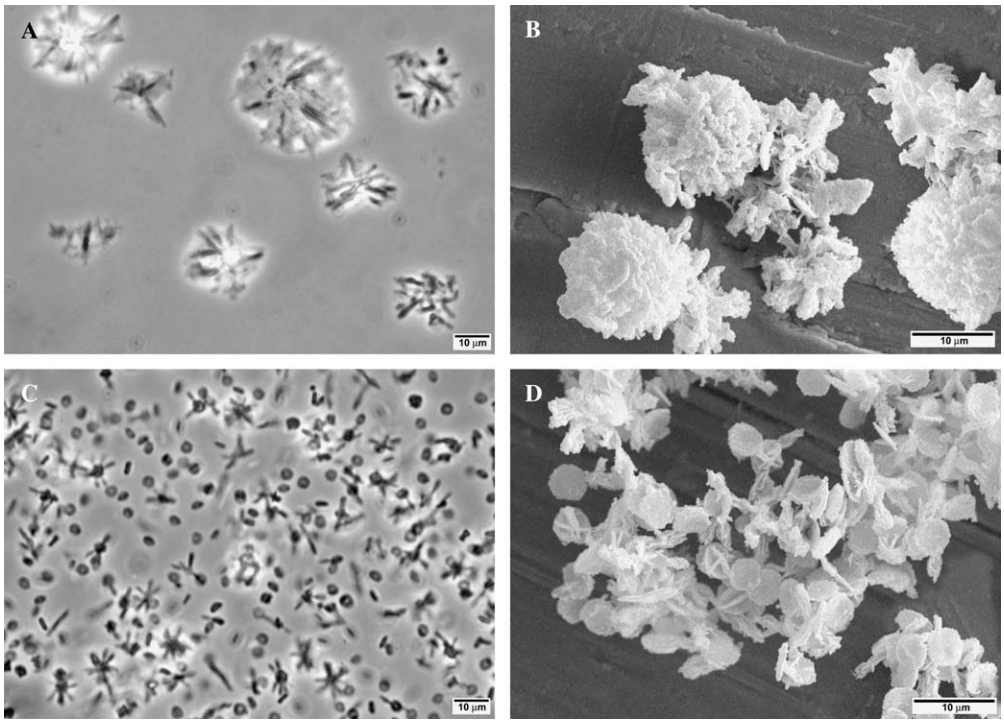

Fig. 7. Micrographs of spherulite fractions formed with myristic acid (Experiment 10, Table 1). (A and C) are phase contrast images. (B and D) are SEM images. (A and B) Images of the large-particle fraction. (C and D) Images of the small-particle fraction.

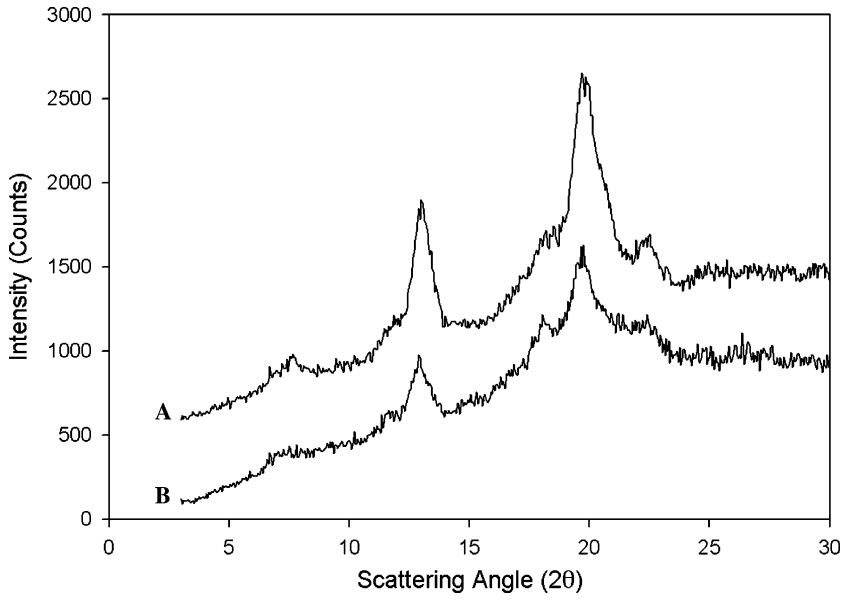

Fig. 8. X-ray powder diffraction scans of spherulites formed with myristic acid (Experiment 10, Table 1). (A) Diffraction scan of the small-particle fraction. (B) Diffraction scan of the large-particle fraction.

importance of the combined effects of the rates of spherulite nucleation and spherulite growth on the determination of spherulite structure. The importance of the fatty acid/amylose ratio was shown in experiments carried out with *n*-propionic acid by Takeo, Tokumura, and Kuge (1973). These authors obtained complexes that exhibited both 6_1 V and 7_1 V diffraction patterns, depending on the relative amounts of amylose and propionic acid used. Additional research is needed to determine the importance of these different variables.

Acknowledgments

We are grateful to Dr. A.R. Thompson for scanning electron micrographs and to J.K. Lingenfelter for technical assistance.

References

Abo el Maaty, M. I., Hosier, I. L., & Bassett, D. C. (1998). A unified context for spherulite growth in polymers. *Macromolecules, 31*, 153–157.

Bassett, D. C. (1984). Electron microscopy and spherulitic organization in polymers. *CRC Critical Reviews in Solid State and Materials Science, 12*(2), 97–163.

Bassett, D. C. (1999). On spherulite growth and cellulation in polymers. A unified context. *Polymer Journal, 31*, 759–764.

Davies, T., Miller, D. C., & Procter, A. A. (1980). Inclusion complexes of free fatty acids with amylose. *Starch/Starke, 32*, 149–158.

Fanta, G. F., Felker, F. C., & Shogren, R. L. (2002). Formation of crystalline aggregates in slowly-cooled starch solutions prepared by steam jet cooking. *Carbohydrate Polymers, 48*, 161–170.

Fanta, G. F., Felker, F. C., Shogren, R. L., & Knutson, K. A. (2001). Starch–paraffin wax compositions prepared by steam jet cooking. Examination of starch adsorbed at the paraffin–water interface. *Carbohydrate Polymers, 46*, 29–38.

Fanta, G. F., Shogren, R. L., & Salch, J. H. (1999). Steam jet cooking of high amylose starch-fatty acid mixtures. An investigation of complex formation. *Carbohydrate Polymers, 38*, 1–6.

Heinemann, C., Escher, F., & Conde-Petit, B. (2003). Structural features of starch–lactone inclusion complexes in aqueous potato starch dispersions: the role of amylose and amylopectin. *Carbohydrate Polymers, 51*, 159–168.

Heinemann, C., Zinsli, M., Escher, F., & Conde-Petit, B. (2003). Influence of starch–flavor interactions on structural properties of aqueous starch dispersions. *Special Publication-Royal Society of Chemistry, 284*, 361–367 (Food Colloids, Biopolymers and Materials).

Kalinka, G., & Hinrichsen, G. (1997). Two-dimensional computer simulation of spherulite formation by branching lamellae. *Acta Polymer*, 256–261.

Klem, R. E., & Brogley, D. A. (1981). Methods for selecting the optimum starch binder preparation system. *Pulp and Paper, 55*, 98–103.

Manley, R. St. J. (1964). Chain folding in amylose crystals. *Journal of Polymer Science: Part A, 2*, 4503–4515.

Morrison, W. R. (1988). Lipids in cereal starches: A review. *Journal of Cereal Science, 8*, 1–15.

Peterson, S. C., Fanta, G. F., Adlof, R. O., & Felker, F. C. (2005). Identification of complexed native lipids in crystalline aggregates formed from jet cooked cornstarch. *Carbohydrate Polymers, 61*, 162–167.

Raphaelides, S., & Karkalas, J. (1988). Thermal dissociation of amylose–fatty acid complexes. *Carbohydrate Research, 172*, 65–82.

Takeo, K., Tokumura, A., & Kuge, T. (1973). Complexes of starch and its related materials with organic compounds. *Stärke, 25*, 357–388.

Yamashita, Y. (1965). Single crystals of amylose V complexes. *Journal of Polymer Science: Part A, 3*, 3251–3260.

Yamashita, Y., & Hirai, N. (1966). Single crystals of amylose V complexes. II. Crystals with 7_1 Helical Configuration. *Journal of Polymer Science: Part A-2, 4*, 161–171.